New Features Extraction and Application based on Gaussian-Hermite Moments in Fingerprint Classification

Lin Wang and Mo Dai

Institute EGID-Bordeaux 3, University of Michel de Montaigne - Bordeaux 3
1 Allée Daguin 33607 Pessac cedex, France
(wang@egid.u-bordeaux.fr and dai@egid.u-bordeaux.fr)

ABSTRACT

Fingerprint classification is an important stage in automatic fingerprint identification systems (AFIS). Key to this process is feature extraction. For fingerprint images, there are two special features singular points (SPs) — core and delta points. Most current classification methods, no matter what they are, structural methods or network-based methods, are based on the extraction of such singular points. In this paper, we propose a new algorithm for the features extraction in fingerprint, which is based on the distribution of Gaussian-Hermite moments of different orders in the fingerprint image. Unlike the common method, we classify the singular points into three types. With these features, we propose a method for fingerprint classification. This method has been tested on the NIST special fingerprint database 4. For the 4000 images in this database, the classification accuracy reaches 87.2 % for the 5-class problem.

1. INTRODUCTION

In recent years, fingerprints are widely used for personal identification. Fingerprint classification is an important stage in automatic fingerprint identification systems (AFIS) because it significantly reduces the time taken in identification of fingerprints, especially where accuracy and speed are critical. Key to this process is feature extraction. However, due to imperfections in the capture of fingerprint images, including the NIST-4 database [1] used by many researchers, feature extraction techniques are prone to errors. For fingerprint images, there are two special features (singular points (SPs)) —core and delta points, and they are highly stable and also rotation- and scale-invariant. Henry classes [2], which classify the fingerprint images into arch, tented arch, left loop, right loop or whorl (see Figure 1), are defined by using the accurate position and type of such singular points. Most current classification methods, no matter what they are, structural methods or network-based methods, are based on the extraction of such singular points [3-8].

(a) Arch (A) (b) Tented arch (T) (c) Left loop (L)

(e) Right loop (R) (f) Whorl (W)

Figure 1. Henry classes

Karu et. al.[4] gives the common rules of classification by the singular points (see Table 1).

Table 1. Fingerprint pattern classes and the corresponding number of singular points

Pattern class	Core	Delta
Arch (A)	0	0
Tented arch (T)	1	1 (middle)
Left loop (L)	1	1 (right)
Right loop (R)	1	1 (left)
Whorl (W)	2	2

While the quality of the fingerprint images varies a lot due to noise, and even in one image, different regions show different quality. So, it is extremely hard to classify such images according to the rules in Table 1.

A common technique to extract SPs in fingerprint is to use the *Poincaré index* introduced by [6]. It is obtained by summing the change in orientation following a closed curve counterclockwise around a point. This technique has been used in [4, 6-8] to extract SPs for fingerprint

classification. However the algorithms based on *Poincare index* may ignore core-delta pairs which are close to each other.

We propose a new features extraction scheme based on moments Gaussian-Hermite for fingerprint classification. With these features, we give a method of fingerprint classification.

In the following sections, we will present the details of our fingerprint classification approach. Section 2 presents Gaussian-Hermite moments (GHM) and their behaviors. Section 3 presents the singular points detection method. In Section 4, we present our classification scheme. In Section 5, we present our experiment results tested on the NIST-4 database. The conclusions are presented in Section 6.

2. GAUSSIAN-HERMITE MOMENTS AND THEIR BEHAVIORS

Moments, such as geometric moments and orthogonal moments, are widely used in pattern recognition, image processing, computer vision and multiresolution analysis. In order to better represent local characteristics in noisy images, the smoothed orthogonal GHM were proposed [9, 10].

2D orthogonal GHM of order *(p, q)* of an input image $I(x, y)$ can be defined:

$$M_{p,q}(x,y,I(x,y))=\iint_{-\infty}^{\infty} G(t,v,\sigma)H_{p,q}(t/\sigma,v/\sigma)I(x+t,y+v)dtdv \quad (1)$$

where $G(t,v,\sigma)$ is the 2D Gaussian function, and $H_{p,q}(t/\sigma,v/\sigma)$, the scaled 2D Hermite polynomial of order *(p, q)*, defined as

$$H_{p,q}(t/\sigma,v/\sigma)=H_p(t/\sigma)\times H_q(t/\sigma) \quad (2)$$

with

$$H_n(x)=(-1)^n\exp\left(-x^2\right)\times\left[\frac{d^n}{dt^n}\left(\exp\left(-x^2\right)\right)\right]$$

Figure 2 shows the spatial responses of the bidimensional GHM kernels of different orders. From Figure 2, we can see that with the increase of the order of the moment base functions, oscillations of the moment base function also increase. This implies that the GHM kernels of different orders characterize different spatial modes.

In fact, GHM are linear combinations of different order derivatives of the signal filtered by a Gaussian filter. As is well known, the derivatives have been extensively used for image representation in pattern recognition. Fingerprint images can be considered as oriented texture patterns. The SPs can thus be regarded as different modes. That is why we use GHM to better extract SPs.

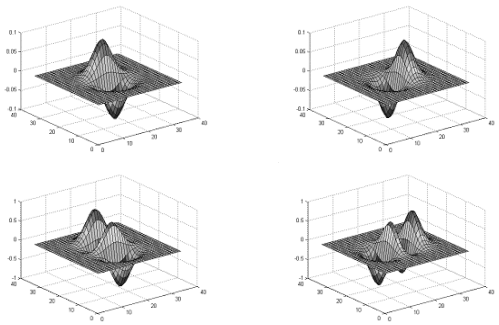

Figure 2. 2D Gaussian-Hermite base functions (orders: (0,1), (1, 0), (0, 3) and (3, 0))

3. FINGERPRINT FEATURE EXTRACTION

Since in a local region, fingerprint mainly consists of parallel ridge and valley structures, the coherence in a region of interest (ridges and valleys of fingerprint impressions) would be higher than that in noisy areas and blank areas. In order to characterize the image by the GHM, using the orthogonality of the GHM, we take the GHM $M_{0,1}$, $M_{1,0}$, $M_{0,3}$ and $M_{3,0}$ to represent the fingerprint image. We define:

$$\begin{cases} M_u(x,y)=\lambda M_{1,0}+(1-\lambda)M_{3,0} \\ M_v(x,y)=\lambda M_{0,1}+(1-\lambda)M_{0,3} \end{cases} \quad (3)$$

where λ ($0<\lambda<1$) is the weight associated with the GHM of different orders of the fingerprint image. For each pixel (x, y) of the fingerprint image, we thus obtain a characteristic vector $[M_u, M_v]^T$ by (3). Figure 3 shows the distribution of $[M_u, M_v]^T$ in a region of interest (foreground), a SP area and a blank area (background) respectively.

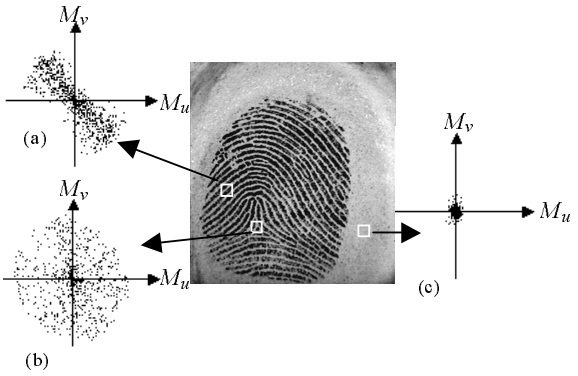

Figure 3. Distribution of $[M_u, M_v]^T$ in a region of interest (a), a SP area (b) and a blank area (c) (window of size 32×32, λ=0.5)

As is shown in Figure 3, in a region of interest, the distribution of $[M_u, M_v]^T$ is along the direction orthogonal to the local ridge orientation. However, in a SP area or a blank area, the distribution of $[M_u,M_v]^T$ is almost a uniform distribution over all directions. So using this behavior of the distribution of $[M_u,M_v]^T$, we can distinguish SPs. We use the principal component analysis (PCA) to analyze the distribution of $[M_u,M_v]^T$. The estimate of the covariance matrix $\boldsymbol{C_M}$ of the vectors $[M_u,M_v]^T$ is given by:

$$\mathbf{C}_{\mathrm{M}}=\begin{bmatrix} \sum_{W}(M_u-m_u)^2 & \sum_{W}(M_u-m_u)(M_v-m_v) \\ \sum_{W}(M_u-m_u)(M_v-m_v) & \sum_{W}(M_v-m_v)^2 \end{bmatrix} \tag{4}$$

with $m_u=\frac{1}{n\times n}\sum_{W}M_u$ and $m_v=\frac{1}{n\times n}\sum_{W}M_v$, where $n\times n$ is the size of the window W.

Let λ_1 and λ_2 be the eigenvalues of the covariance matrix $\boldsymbol{C_M}$. When $\lambda_1 >> \lambda_2$, the distribution of $[M_u,M_v]^T$ will be mainly along the long axis, i.e., in the direction orthogonal to the orientation of ridges; on the contrary, in a noisy area and SP area, λ_2 will be close to λ_1. Therefore we can define the coherence as follows:

$$coherence=\frac{\lambda_1-\lambda_2}{\lambda_1+\lambda_2}=\frac{\sqrt{\left(\sum_{W}(M_u-m_u)-\sum_{W}(M_u-m_u)\right)^2+4\left(\sum_{W}(M_u-m_u)(M_v-m_v)\right)^2}}{\sum_{W}(M_u-m_u)^2+\sum_{W}(M_v-m_v)^2} \tag{5}$$

As a byproduct, we also obtain the local ridge orientation of the point (x_i, y_i) by the eigenvector of the covariance matrix $\boldsymbol{C_M}$ that belongs to the largest eigenvalue λ_1.

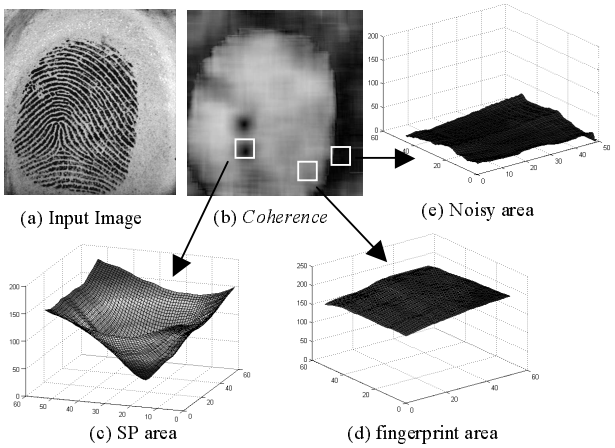

Figure 4. Images function of *coherence* in different areas of the fingerprint

Figure 4 shows a fingerprint image and its *coherence* image (shown as grayscale image). It can be clearly seen that the *coherence* is close to 1 in the significant area of the fingerprint, while it is close to 0 and at the same time is a local minimum in a SP. The image function of *coherence* in a SP area approximates a taper (see Figure 4(c)). Although *coherence* in a noisy area also is very low, it is not local minimum (see Figure 4(e)).

To find the position of a possible SP, the local minimum is extracted in *coherence* image. If *coherence*(x_i, y_i) is the local minimum, a SP is found at point (x_i, y_i). Figure 5 shows the results of detection SPs by proposed algorithm in two fingerprint images. All of the SPs were accurately detected in these fingerprint images, especially a core-delta pair where a core and a delta are close to each other (see Figure 5(b)). In other methods, such core-delta pair often is ignored.

Figure 5. Results of detection SPs by proposed method in two fingerprint images

Unlike common methods that classify SPs into two types (core and delta) by *Poincaré Index*, in our algorithm, SPs are classified into three types (denoted S_1, S_2, and S_3 respectively) by the dominant directions around SP. Figure 6 shows three type of SP.

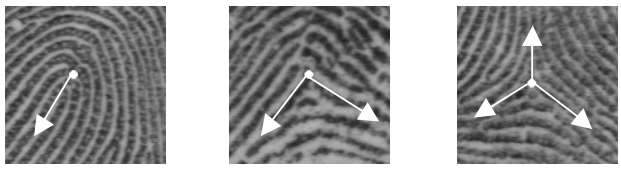

Figure 6. Three type SPs: (a) S_1, (b) S_2, and (c) S_3

In order to search the dominant direction of SP, The sampling points assigned to each SP can be organized in a circular pattern around the SP position P=(x,y), as illustrated in Figure 7. The circular pattern consists of K sampling points P_k ($1\le k\le K$), equally distributed along its circumference. Denoting by θ_k the local ridge orientation estimated in P_k, we define the SP descriptor as follows:

$$f(k)=\left|\sin(\theta_k-d_k)\right| \tag{6}$$

with $d_k = 2(k-1)\pi / K$

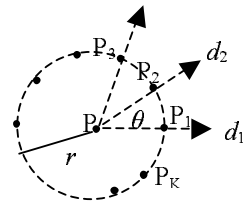

Figure 7. Sampling points organized in a circular pattern around a SP

Finally, we use Gaussian smoothing operator to smooth f in a neighborhood. In our experiment, we take K=32. Figure 8 shows f of three types of SPs respectively.

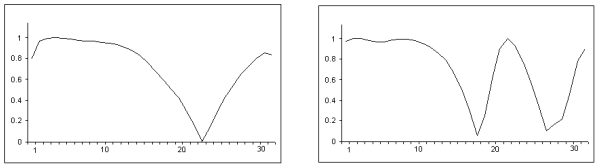

(a) f of S_1 (b) f of S_2

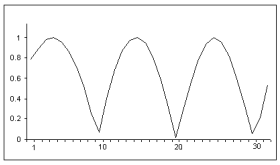

(c) f of S_1

Figure 8. f of three types of SPs

The dominant direction of SP can be obtained by search the local minimum.

4. CLASSIFICATION RULES

After all the necessary steps having been carried out, we will decide to which class the image belongs. The classification rules are as follows (N_i is the number of S_i (i=1, 2, 3)):

(1) If N_1>= 2, a whorl is assigned;

(2) If $N_1=N_2=N_3=0$, an arch is assigned to the image;

(3) If $N_1=N_3=0$, $N_2=1$, a tended arch is assigned to the image;

(4) If ($N_1=N_3=1$), or ($N_1=N_2=1$ and $N_3=0$), analyze S_1/S_3 or S_1/S_2 pair according to the following rules:

- Calculate the difference $\Delta\theta$ between the dominant direction θ_1 of S1 and the direction θ' pointing from the point S_1 to the point S_3 (or S_2) (see Figure 9):

$$\Delta\theta = \begin{cases} \theta' - \theta_1 & |\theta' - \theta_1| < \pi \\ \theta' - \theta_1 - 2\pi & \theta' - \theta_1 \geq \pi \\ \theta' - \theta_1 + 2\pi & \theta' - \theta_1 \leq -\pi \end{cases} \quad (7)$$

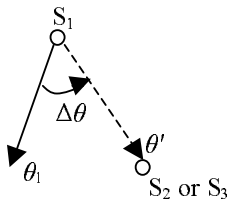

Figure 9. Illustration of the difference $\Delta\theta$

- Then the class is determined as follows:

$$\text{class} = \begin{cases} \text{L} & \Delta\theta > \pi/12 \\ \text{T} & |\Delta\theta| \leq \pi/12 \\ \text{R} & \Delta\theta < -\pi/12 \end{cases} \quad (8)$$

where T means a tented arch, L a left loop, R a right loop.

(5) If N_1=1 and $N_2=N_3=0$, calculate the difference between the dominant direction of this SP and the direction of ridges (see Figure 10).

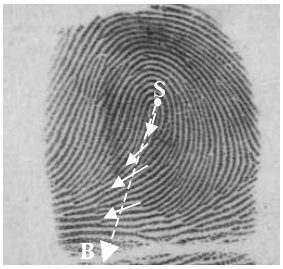

Figure 10. Local direction following the dominant direction

More precisely, denoting the SP by S, we start from S and follow the dominant direction until meeting boundary of the image at point B (see Figure 10). Let β be the dominant direction of SP, and let $\alpha_1, \alpha_2, \ldots, \alpha_n$ be the local direction angles on the line segment SB. We define the averaged sum as follow:

$$\Delta = \frac{1}{n}\sum_{i=1}^{n} d(\alpha_i, \beta) \quad (9)$$

with

$$d(\alpha,\beta) = \begin{cases} ((\alpha-\beta) \bmod \pi) & \text{if } |((\alpha-\beta) \bmod \pi)| < \pi/2 \\ ((\alpha-\beta) \bmod \pi) + \pi & \text{if } |((\alpha-\beta) \bmod \pi)| \leq -\pi/2 \\ ((\alpha-\beta) \bmod \pi) - \pi & \text{if } |((\alpha-\beta) \bmod \pi)| \geq \pi/2 \end{cases}$$

The class is assigned as follows:

$$\text{Class} = \begin{cases} \text{L} & \Delta < -\pi/12 \\ \text{T} & |\Delta| \leq \pi/12 \\ \text{R} & \Delta > \pi/12 \end{cases} \quad (10)$$

(6) If N_3=1 and N_1=N_2=0, the rule is similarly obtained to (5):

$$\text{Class} = \begin{cases} \text{L} & \Delta > -\pi/12 \\ \text{T} & |\Delta| \le \pi/12 \\ \text{R} & \Delta < \pi/12 \end{cases} \quad (11)$$

(7) Otherwise, the class is unknown.

5. EXPERIMENT RESULTS

The NIST special fingerprint database 4 (NIST-4) [1] we use in our experiment contains 4000 fingerprint images, and the five classes (L=left loop, R=right loop, W=whorl, T=tented arch, and A = arch) are evenly distributed. For all the 4000 images in the database, the 5-class results of our algorithm are shown in Table 2. From this table, we obtain that the 5-class classification result is 87.2% without rejection. Table 3 shows the results of the algorithm [7] in the same fingerprint database. It can be obtained that the 5-class classification rate is 84.3% without rejection.

Table 2. Five-class experimental results with our algorithm tested on NIST and no rejection

True Class	Assigned Class					
	Left loop	Right loop	Whorl	Tented arch	Arch	Unknown
Left loop	722	11	23	6	48	5
Right loop	15	706	30	8	50	8
Whorl	25	27	725	5	5	8
Tented arch	35	17	14	429	136	5
Arch	9	7	3	9	905	4

Table 3. Five-class experimental results with the algorithm [7] tested on NIST and no rejection

True Class	Assigned Class					
	Left loop	Right loop	Whorl	Tented arch	Arch	Unknown
Left loop	739	5	25	0	44	2
Right loop	14	721	24	3	51	4
Whorl	27	26	727	5	3	7
Tented arch	31	12	18	278	293	4
Arch	7	6	4	11	908	1

From these tables, we can see that our algorithm is better than the algorithm [7] for distinguishing tented arch. Figure 11 shows two examples of fingerprint image. In the fingerprints (a) and (b), our algorithm can correctly classify, while the algorithm [7] cannot correctly class.

(a) (b)

Figure 11. Our algorithm: (a) and (b) correctly classified;
Algorithm [7]: (a) a left loop as an arch, (b) a tended arch as an arch.

Figure 12 is a misclassified fingerprint with both our algorithm and algorithm [7].

Figure 12. A misclassified fingerprint with both two algorithms.

6. CONCLUSION

For fingerprint classifications, the traditional structural methods are based on the detection of the singular points as core or delta points by the analysis of the orientation field.

In this paper, we propose a new algorithm for the extraction of singular point in fingerprint, which is based on the distribution of Gaussian-Hermite moments of different orders in the fingerprint image. Unlike the traditional structural methods, we classify the singular points into three types. With these features, we propose a method for fingerprint classification. This method has been tested on the NIST-4. For the 4000 images in this database, the classification accuracy reaches 87.2 % for the 5-class problem. In the comparison with algorithm [7], our method has performed better.

REFERENCES

[1] C. I. Watson and C. L. Wilson, "NIST Special Database 4, Fingerprint Database," *National Institute of Standards and Technology, March*, 1992.

[2] E. R. Henry, *Classification and uses of Fingerprints*. London, Routledge, 1901.

[3] R. Cappelli, A. Lumini, D. Maio, and D. Maltoni, "Fingerprint classification by directional image partitioning," *Transactions on Pattern Analysis Machine Intelligence*, vol. 21, pp. 402–421, 1999.

[4] K. Karu and A. Jain, "Fingerprint classification," *Pattern Recognition*, vol. 29, pp. 389-404, 1996.

[5] A. K. Jain, S. Prabhakar, and L. Hong, "A multi-channel approach to fingerprint classification," *IEEE Trans. Pattern Anal. Machine Intelligence*, vol. 21, pp. 348-359, 1999.

[6] M. Kawagoe and A. Tojo, "Fingerprint pattern classification," *Pattern Recognition*, vol. 17, pp. 295-303, 1984.

[7] Q. Zhang and H. Yan, "Fingerprint classification based on extraction and analysis of singularities and pseudo ridges," *Pattern Recognition*, vol. 37, pp. 2233-2243, 2004.

[8] H. O. Nyongesa, S. AL-Khayatt, S. M. Mohamed, and M. Mahmoud, "Fast Robust Fingerprint Feature Extraction and Classification," *Journal of Intelligent and Robotic Systems*, vol. 40, pp. 103–112, 2004.

[9] J. Shen, "Orthogonal Gaussian-Hermite Moments for Image Characterization," in: Proc. SPIE, Intelligent Robots and Computer Vision XVI: Algorithms Techniques, Active Vision, and Materials Handling, Pittsburgh, USA, 1997.

[10] J. Shen, W. Shen, and D. F. Shen, "On geometric and orthogonal moments," *International Journal of Pattern Recognition and Artificial Intelligence*, vol. 14, pp. 875-894, 2000.